

The obscured QSO 1SAX J1218.9+2958

N.S. Loaring¹ \star , M.J. Page¹, G. Ramsay¹

¹*Mullard Space Science Laboratory, University College London, Dorking, Surrey, RH5 6NT, UK*

2 February 2008

ABSTRACT

We present results from *XMM-Newton* observations of the obscured QSO 1SAX J1218.9+2958. We find that the previously reported optical and soft X-ray counterpart positions are incorrect. However we confirm the spectroscopic redshift of 0.176. The optical counterpart has a K magnitude of 13.5 and an R–K colour of 5.0 and is therefore a bright extremely red object (ERO). The X-ray spectrum is well described by a power-law ($\Gamma = 2.0 \pm 0.2$) absorbed by an intrinsic neutral column density of $8.2^{+1.1}_{-0.7} \times 10^{22} \text{ cm}^{-2}$. We find that any scattered emission contributes at most 0.5 percent to the total X-ray flux. From the optical/near-IR colour we estimate that the active nucleus must contribute at least 50 percent of the total flux in the K band and that the ratio of extinction to X-ray absorption is 0.1 – 0.7 times that expected from a Galactic dust-gas ratio and extinction curve. If 1SAX J1218.9+2958 were $100\times$ less luminous it would be indistinguishable from the population responsible for most of the 2–10 keV X-ray background. This has important implications for the optical/IR properties of faint absorbed X-ray sources.

Key words: galaxies: active – X-rays: galaxies – X-rays: diffuse background

1 INTRODUCTION

The cosmic X-ray background (XRB) is the combined X-ray emission from all extragalactic X-ray source populations, integrated over cosmic time. Surveys made using *ROSAT* resolved 70–80 percent of the XRB into discrete sources (Hasinger et al., 1998) at soft energies (0.5–2.0 keV). The majority of these sources are QSOs and Seyfert 1 galaxies: unobscured active galactic nuclei (AGN) with broad emission lines (McHardy et al., 1998; Lehmann et al., 2001). However, the XRB cannot be explained solely by extrapolating these sources to fainter fluxes as their spectra are softer than that of the XRB. To reproduce the XRB spectrum, an additional population of faint hard sources is required. Leading X-ray background synthesis models identify the faint hard sources with intrinsically absorbed AGN (Comastri et al., 1995; Wilman et al., 2000; Gilli et al., 2001). The absorbed AGN are expected to constitute 80 to 90 percent of the total AGN population (Fabian & Iwasawa, 1999).

The anticipated population of faint, hard sources has now been detected in *Chandra* and *XMM-Newton* surveys (Tozzi et al., 2001; Brandt et al., 2001; Hasinger et al., 2001). However, even before the launch of *XMM-Newton* and *Chandra*, a number of X-ray surveys

were carried out using *ROSAT*, *ASCA*, and *BeppoSAX* to investigate the absorbed AGN population (Ueda et al., 1999; Fiore et al., 1999; Page et al., 2000). These surveys covered large areas of sky and so were particularly useful for finding relatively bright, and thus easily studied, examples of the absorbed AGN population.

The sources detected in these surveys exhibit interesting, and somewhat surprising properties. For example, Maiolino et al. (2000) found that AGN from the *BeppoSAX* High Energy Large Area Survey (HELLAS) could be divided into two groups according to their optical and near-IR properties. One group of sources have point-like optical/near-IR counterparts with colours typical of optically selected QSOs. The other group of sources are extended in the optical/near-IR and have colours dominated by the host galaxy stellar population. Despite having a wide range of X-ray absorbing column densities up to 10^{23} cm^{-2} , none of the sources studied by Maiolino et al. (2000) appeared to have colours dominated by a reddened AGN.

Comparison of *ROSAT* and *BeppoSAX* data on HELLAS sources yielded another unexpected result: Vignali et al. (2001) found that a significant fraction of the absorbed objects in HELLAS have an additional soft component in their X-ray spectra. This could be due to scattered X-rays which do not pass through the absorber, alternatively it might indicate a hot gas component as observed in starburst galaxies.

Perhaps one of the most puzzling results is that

\star nsl@mssl.ucl.ac.uk

in many AGN whose X-ray spectra indicate a substantial absorbing column ($> 10^{22} \text{ cm}^{-2}$), the corresponding optical spectrum shows little or no evidence for dust reddening (Akiyama et al., 2000; Page et al., 2001; Comastri et al., 2001). This suggests that the absorbing media of AGN typically have much lower dust-gas ratios than the interstellar medium of our Galaxy (Maiolino et al., 2001a).

Observations of hard X-ray selected, absorbed AGN have the potential to reveal much about the dominant, absorbed XRB-producing population of AGN. Here we report new X-ray and optical observations of the HELLAS source 1SAX J1218.9+2958, an absorbed X-ray source, optically classified as a Seyfert 1.9 galaxy (Fiore et al., 1999). It has a broad component to its $\text{H}\alpha$ emission line (hence the Seyfert 1.9 classification) but its optical/near-IR colours appeared to be completely dominated by its host galaxy (Maiolino et al., 2000). It was proposed to have a *ROSAT* counterpart, (and thus a significant soft X-ray excess) by Vignali et al. (2001).

Throughout this paper we assume a flat ΛCDM cosmology with $(\Omega_M, \Omega_\Lambda) = (0.3, 0.7)$ and a Hubble constant of $70 \text{ km s}^{-1} \text{ Mpc}^{-1}$.

2 OBSERVATIONS AND DATA REDUCTION

2.1 *XMM-Newton* data

1SAX J1218.9+2958 is a serendipitous source in two *XMM-Newton* observations of Markarian 766. The first observation was performed on 20th May 2000 and had an exposure time of 28 ks in EPIC MOS (an intermediate resolution X-ray imaging spectrometer, Turner et al., 2001).

The second observation took place exactly one year later, with a MOS exposure time of 127 ks. In both observations the EPIC PN camera was operated in small window mode, and hence did not record any data for 1SAX J1218.9+2958.

The data were processed using the *XMM-Newton* Science Analysis System (SAS) v5.3. Periods of high background in the 2001 observation were excised from the event lists, to leave 95 ks of useful exposure time. There were no periods of high background during the May 2000 observation, so the total useful exposure time of the two observations is 123 ks. At an off axis angle of 8.6 arc minutes, this corresponds to an effective exposure time of 82 ks at 2 keV.

For the purpose of obtaining an accurate source position, images and exposure maps were constructed in the energy band 1–10 keV. These images were source searched using the SAS routines EBOXDETECT and EMLDETECT. A linear shift of ~ 2 arc seconds, based on the relative position of Markarian 766 in the EPIC images and the 2MASS catalogue, was applied to the X-ray position of 1SAX J1218.9+2958 to match the optical/IR astrometric reference frame.

We extracted X-ray spectra in the energy range 0.2–12 keV for the source and background from each exposure, including all valid single, double and triple X-ray event patterns. We have used the latest EPIC MOS redistribution matrix files and generated appropriate ancillary response files for our spectra using the SAS task ARFGEN. The source

	RA (J2000) Dec	
<i>XMM-Newton</i>	12:18:54.73	+29:58:06.6
APM	12:18:54.71	+29:58:06.7
2MASS	12:18:54.68	+29:58:06.7

Table 1. X-ray, optical and IR positions of 1SAX J1218.9+2958

has a similar countrate and similar X-ray spectrum in both observations. Therefore the spectra from both observations and both MOS cameras were co-added to maximise signal to noise. Finally, the resulting spectrum was grouped to a minimum of 50 counts per channel.

2.2 Optical/IR data

The online APM¹ and 2MASS² databases were used to find the optical/IR counterpart for 1SAX J1218.9+2958. In addition, an I band image was obtained in January 2002 during photometric conditions using the Andalucia Faint Object Spectrograph and Camera (ALFOSC) on the Nordic Optical Telescope (NOT). An optical spectrum of 1SAX J1218.9+2958 was also obtained using ALFOSC in January 2002. A ten minute integration was taken using Grism 4 (3200–9100 Å) with a slit 1.8 arc sec wide providing a resolution of 23 Å. Relative flux calibration was determined from an observation of the standard star Feige 66.

3 THE X-RAY POSITION OF 1SAX J1218.9 + 2958 AND IDENTIFYING THE OPTICAL/IR COUNTERPART

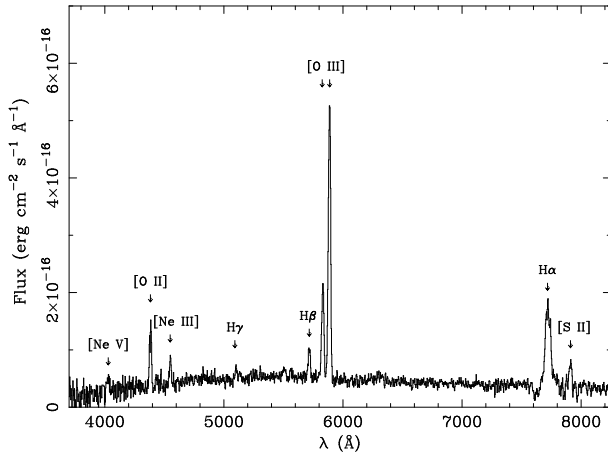
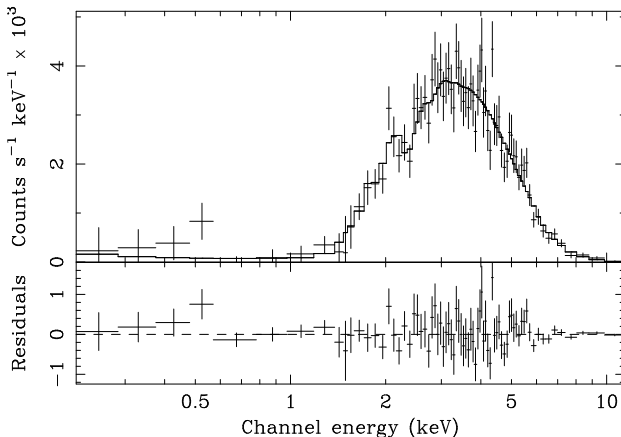
The *XMM-Newton* derived position for 1SAX J1218.9+2958 is given in Table 1. The statistical uncertainty on this position is sub-arc second, and the systematic uncertainty is ~ 1 arc sec (Watson et al., 2001), a significant improvement upon the ~ 1 arc minute uncertainty of the HELLAS position (Fiore et al., 1999).

At the X-ray position we find unambiguous counterparts in the APM and 2MASS catalogues, and their positions are given in Table 1. There is no corresponding *ROSAT* counterpart. We provide a summary of the optical/IR counterpart's photometric properties in Table 2. The spectrum of the optical counterpart is shown in Figure 1. It is a Seyfert 1.9 galaxy at a redshift $z = 0.176$. The position of the optical counterpart reported by the HELLAS team (Fiore et al., 1999; Maiolino et al., 2000; La Franca et al., 2002) is incorrect. However, the spectrum of the optical counterpart shown in Fiore et al. (1999) has exactly the same emission line ratios as seen in our NOT spectrum. Subsequently we have learned that the spectrum and redshift given by Fiore et al. (1999) are in fact for the correct optical counterpart, but the reported co-ordinates were mistakenly given for a second object observed simultaneously through the same slit (A. Comastri, private communication).

¹ <http://www.ast.cam.ac.uk/~mike/apmcat/>

² <http://www.ipac.caltech.edu/2mass/>

2MASS		POSS	POSS	NOT		2MASS	
RA (J2000)	Dec	O (B)	E (R)	I	J	H	K
12 18 54.68	+29 58 06.7	20.07 (19.88)	18.52 (18.52)	17.95±0.1	16.425	14.935	13.499

Table 2. Optical and IR colours of the source.**Figure 1.** Optical spectrum of 1SAX J1218.9+2958. Prominent emission lines are marked for $z = 0.176$.**Figure 2.** The top panel shows the observed EPIC MOS spectrum of 1SAX J1218.9+2958 (datapoints) fitted with an absorbed power law model (histogram). The bottom panel shows the residuals to the model fit.

4 X-RAY SPECTRAL ANALYSIS

We have used XSPEC v11.2 to analyze the X-ray spectrum. The results described in this section are given in Table 3 and all errors on the fit parameters are quoted at 90 per cent confidence for one interesting parameter ($\Delta\chi^2 = 2.706$).

4.1 Absorbed power-law model

The spectrum is shown in Figure 2; the low count rate below 1 keV implies that the spectrum is heavily absorbed. We therefore fitted an absorbed power-law model. A Galac-

tic component to the absorption model was included, with $N_H = 1.7 \times 10^{20} \text{ cm}^{-2}$, (Dickey & Lockman, 1990). This simple model is a good fit to the data and is overplotted in Figure 2. The best fit power-law photon index is $\Gamma = 2.0 \pm 0.2$, and the best fit column density intrinsic to 1SAX J1218.9+2958 is $8.2_{-0.7}^{+1.1} \times 10^{22} \text{ cm}^{-2}$. The observed 2–10 keV flux is $8.6 \times 10^{-13} \text{ erg s}^{-1} \text{ cm}^{-2}$, with a corresponding unobscured rest frame 2–10 keV luminosity of $1.1 \pm 0.1 \times 10^{44} \text{ erg s}^{-1}$.

4.2 Reflection and reprocessing

Reprocessing of the primary power-law radiation by cold material will result in a Fe K_α emission line at 6.4 keV and a reflected component, which has an Fe K edge at 7.1 keV (George & Fabian, 1991; Matt, Perola & Piro, 1991). Addition of a narrow line at a rest frame energy of 6.4 keV does not produce a significant improvement to the fit. Adding a cold reflection component also results in an insignificant improvement in fit. The reflection component is poorly constrained and the 90 percent upper limit to the equivalent width of the Fe K_α line (111 eV) is compatible with the typical level of reflection seen in Seyfert 1 galaxies (Nandra et al., 1997) and with the reprocessing expected in the absorbing medium (Leahy & Creighton, 1993).

Some Seyfert 2 galaxies show broad optical emission lines in polarised light (e.g. Antonucci & Miller, 1985), implying that some of the nuclear radiation is scattered into our line of sight without passing through the absorbing medium. We have therefore added a second intrinsically unabsorbed power-law component to our model. This does not significantly improve the fit, and the normalisation of the scattered power-law component is $< 0.5\%$ of the primary, absorbed, power-law component. In several heavily absorbed Seyfert galaxies the spectrum below 1 keV is dominated by emission from photo-ionised gas (Kinkhabwala et al., 2002; Sako et al., 2000). The strongest soft X-ray emission feature in these objects is the OVII triplet of emission lines at rest frame energy of 0.57 keV which is unresolved at the EPIC spectral resolution. Addition of a narrow rest frame 0.57 keV emission line does not significantly improve the fit.

5 AGN CONTRIBUTION TO THE OPTICAL/IR FLUX

The observed IR colours of R–K=5.0, J–H=1.5 and H–K=1.4 are all too red for a spiral or elliptical galaxy at $z = 0.176$, where one would expect R–K=3.1, (Roche et al., 2002), and J–H=0.8, H–K=0.5 (Fioc & Rocca-Volmerange, 1999) suggesting that the dust-reddened nucleus is visible in the near-IR.

We have estimated the relative contribution to the K band flux from the active nucleus as a function of

Model	Γ	Intrinsic N_H (10^{22} cm^{-2})	EW (eV)	Line flux ($10^{-14} \text{ erg cm}^{-2} \text{ s}^{-1}$)	Scattered fraction (%)	R	$\chi^2/\text{d.o.f.}$
Absorbed power-law	$2.0^{+0.2}_{-0.2}$	$8.2^{+1.1}_{-0.7}$					69/73
Absorbed power-law + iron K_α line	$2.0^{+0.3}_{-0.2}$	$8.3^{+1.1}_{-0.7}$	56^{+57}_{-53}	$0.8^{+0.8}_{-0.8}$			66/72
Absorbed power-law + reflection + iron K_α line	$2.3^{+0.3}_{-0.4}$	$8.9^{+0.9}_{-0.8}$	52 ± 52	$0.7^{+0.8}_{-0.7}$		$1.8^{+6.0}_{-1.8}$	66/71
Absorbed power law + scattered component	$2.0^{+0.2}_{-0.2}$	$8.4^{+1.1}_{-0.9}$			$0.2^{+0.3}_{-0.2}$		68/72
Absorbed power-law + OVII line	$2.0^{+0.1}_{-0.1}$	$8.3^{+0.8}_{-0.9}$	-	$0.1^{+0.1}_{-0.1}$			66/72

Table 3. X-ray spectral model fitting results. R is the normalisation of the reflection component compared to a plane reflector covering half of the sky as seen from the central source.

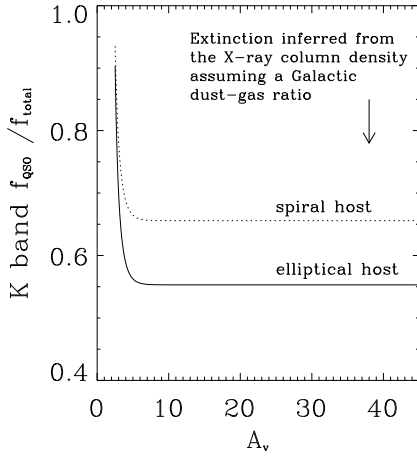


Figure 3. The fractional AGN flux contribution to the total K band flux required to yield the observed B–K colour for different absorbing column densities. Elliptical galaxy; solid line. Spiral galaxy; dashed line.

intrinsic reddening for both elliptical and spiral host galaxy morphologies. This estimate is based on the B–K colour, which has the largest available spectral leverage. We used the elliptical and Sa spiral galaxy templates of Mannucci et al. (2001) and the QSO composite spectrum of Francis et al. (1991) extended to the K band. For a range of extinctions we reddened the QSO composite spectrum assuming that any obscuring matter in the AGN has a Galactic extinction curve (Fitzpatrick, 1999) and determined the relative AGN and galaxy contributions to the total flux required to produce the observed B–K colour.

Figure 3 shows the allowed combinations of nuclear contribution versus intrinsic reddening for an elliptical and for a spiral host. For an elliptical host the relative contribution from the active nucleus is always greater than 55 percent and rises sharply with decreasing absorption. For a spiral host the minimum active nucleus contribution is 66 percent. Regardless of host galaxy morphology or the degree of reddening the AGN makes a substantial contribution to the near-IR flux.

We have also explicitly calculated the B band and K band magnitudes for the host and active nucleus correspond-

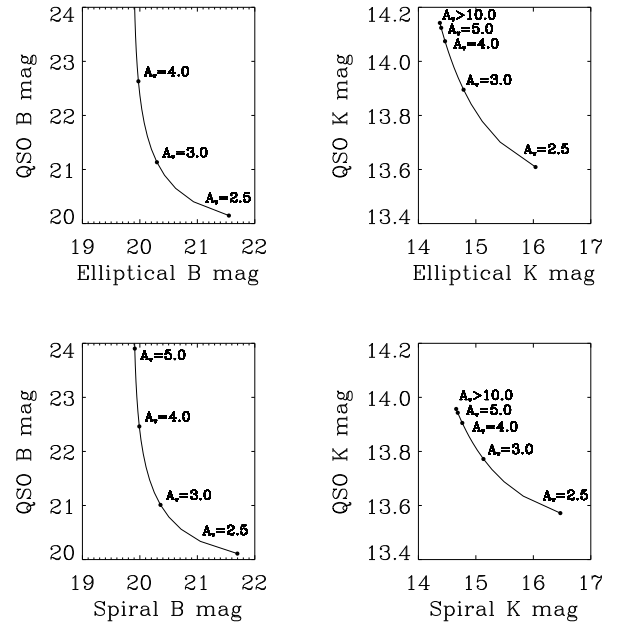


Figure 4. The host galaxy and AGN magnitudes in the B and K bands allowed in order to reproduce the observed B–K colour.

ing to the permitted range of reddening and flux contributions shown in Figure 3. The results are illustrated in Figure 4. As the left panel shows, unless the AGN is reddened by less than $A_v \sim 5$ (equivalent to $N_H \sim 10^{22} \text{ cm}^{-2}$), the host galaxy is responsible for virtually all the B band flux.

6 OPTICAL SPECTRUM

The measured $[\text{OIII}]/\text{H}\beta$ ratio for 1SAX J1218.9+2958 is ~ 10 , of order $20\times$ larger than typically observed in optically selected QSOs. This suggests that 1SAX J1218.9+2958 is extinguished by at least $A_v = 3.3$, corresponding to a minimum equivalent neutral hydrogen column density of $6.5 \times 10^{21} \text{ cm}^{-2}$.

Assuming a galaxy flux contribution of 14 percent in the R band at $z = 0$ for typical unabsorbed AGN (Hutchings, Crampton & Campbell, 1984), we have

matched the observed equivalent width of the broad H_β component in our optical spectrum with that of an obscured QSO plus host galaxy model spectrum. We find an optical extinction of $A_v \geq 4.0$, similar to that derived via the observed $[\text{OIII}]/H_\beta$ ratio. Comparison with our X-ray determined column density of $8.2 \times 10^{22} \text{ cm}^{-2}$ implies that the ratio of optical/IR extinction to X-ray absorption in 1SAX J1218.9+2958 is at least $\frac{1}{10}$ Galactic.

Another estimate of the optical extinction may be derived via the observed optical to X-ray slope, α_{ox}^3 . About 90% of low redshift unobscured QSOs have $1.2 < \alpha_{\text{ox}} < 1.7$ (Laor et al., 1997). Starting from the unabsorbed 0.5–2.0 keV flux ($1.1 \times 10^{-12} \text{ erg cm}^{-2} \text{ s}^{-1}$) we determined the spread of 2500Å flux consistent with this range of α_{ox} , and converted these flux values to B and K band magnitudes using the template of Francis et al. (1991). Taking into account the uncertainty on the measured X-ray flux, we expect unreddened B and K magnitudes of $15.3^{+3.3}_{-1.9}$ and $12.3^{+3.3}_{-1.9}$ respectively. Assuming an AGN contribution of between 50–100 percent in the K band, the observed K band magnitude of 13.5 implies optical extinction in the range $A_v \leq 29$. Combining this upper limit with the lower limit derived from H_β we conclude that the ratio of optical/IR extinction to X-ray absorption in 1SAX J1218.9+2958 is 0.1 – 0.7 Galactic.

7 DISCUSSION

7.1 Dust-gas ratio

A low dust-gas ratio has been observed in several samples of obscured AGN (e.g. Maccacaro et al., 1982; Akiyama et al., 2000; Page et al., 2001). This has been attributed to either a reduced dust content in these AGN, or as a consequence of possible different emission regions, with X-ray emission associated with deeper regions than optical emission (Reichert et al., 1985). Maiolino et al. (2001a) have also found dust-gas ratios significantly lower than the standard Galactic value, for AGN with intrinsic luminosities $> 10^{42} \text{ erg s}^{-1}$. However, they attribute this to a dust grain distribution biased in favour of large grains which flattens the extinction curve (Laor & Draine, 1993) and explains the reduced A_v/N_H and $E(B-V)/N_H$ (Maiolino et al., 2001b). Weingartner & Murray (2002) propose that most of the X-ray absorption in the Maiolino et al. (2001a) galaxies occurs in a region distinct from the region responsible for the optical extinction.

In 1SAX J1218.9+2958 the ratio of optical/IR extinction to X-ray absorption is only 0.1–0.7 times that expected assuming a Galactic dust-gas ratio, in line with these previous studies. As this appears to be a widespread property of absorbed AGN it has important consequences for the optical/IR appearance of the faint X-ray population.

7.2 Implications for the faint source population

Faint X-ray sources with 2–10 keV fluxes of $\sim 10^{-14} \text{ erg s}^{-1}$ are responsible for a large fraction of the X-ray background. At these fluxes a high proportion of the sources

are absorbed, with apparent column densities of $\sim 10^{22} \text{ cm}^{-2}$ (Rosati et al., 2002). In many cases their optical counterparts are extremely red (Barger et al., 2001; Alexander et al., 2002; Crawford et al., 2002), confirming previous *ROSAT* findings (Lehmann et al., 2000, 2001). However, understanding the nature of these sources has proved difficult due to their optical faintness.

For those objects which are too faint for optical spectroscopy, photometric redshifts are estimated assuming that the optical and IR emission is dominated by the host galaxy (Alexander et al., 2002; Lehmann et al., 2001; Franceschini et al., 2001; Crawford et al., 2002). The justification for this assumption comes from the observation that similar sources for which optical spectroscopy is possible are dominated in the optical by their host galaxies (Lehmann et al., 2001), and that the optical to IR colours of the faint sources are consistent with those of elliptical or spiral galaxies (Mainieri et al., 2002; Koekemoer et al., 2002).

However, in 1SAX J1218.9+2958 a dust reddened AGN contributes at least 50 percent of the flux in the K band. 1SAX J1218.9+2958 is similar both in its X-ray spectral properties and in its optical colours to the sources which populate faint X-ray surveys although it is $\sim 100\times$ brighter. At $10^{-14} \text{ erg s}^{-1} \text{ cm}^{-2}$ we expect objects similar to 1SAX J1218.9+2958 to look identical to typical deep field sources and to be about 250 times more numerous on the sky than at a flux of $8.6 \times 10^{-13} \text{ erg s}^{-1} \text{ cm}^{-2}$ (assuming the type 1 luminosity function slope from Page et al., 1997). It is therefore possible that a non-negligible fraction of faint sources could in fact have a significant AGN contribution in the near-IR.

Further evidence that significant numbers of faint absorbed sources have large AGN contributions in the near-IR comes from the recent studies of Gandhi et al. (2002) and Stevens et al. (2003). Stevens et al. (2003) found that three out of five of their X-ray selected EROs are point-like and therefore AGN dominated in the K band, while Gandhi et al. (2002) found three out of eight of their sample of hard *Chandra* sources are point-like and have broad emission lines (i.e. are AGN dominated) in the near-IR.

One significant consequence of the presence of a reddened AGN in the near-IR is that photometric redshift determinations assuming a galaxy spectrum could be inaccurate. Weak, low redshift objects could be assigned high redshifts in order to reproduce the red colours from galaxy templates. An additional AGN contribution to the rest frame near-IR flux should therefore be considered when determining photometric redshifts for sources with similar X-ray column densities to 1SAX J1218.9+2958.

8 CONCLUSIONS

We have presented the hard X-ray and optical spectra of the obscured QSO 1SAX J1218.9+2958. We find that the position reported for the optical counterpart (e.g. Fiore et al., 1999) was incorrect. However, the redshift and optical spectrum given by (Fiore et al., 1999) are correct. The optical counterpart is an extremely red object with $R-K=5.0$ and there is no *ROSAT* counterpart.

The X-ray spectrum is consistent with a Compton thin absorbed power-law of photon index 2.0 ± 0.2 and intrinsic

³ defined as the ratio of the UV flux at 2500Å to that of the X-ray flux at 2keV

column density of $N_H = 8.2^{+1.1}_{-0.7} \times 10^{22} \text{ cm}^{-2}$. The intrinsic 2–10 keV luminosity is $1.1 \pm 0.1 \times 10^{44} \text{ erg s}^{-1}$ which places 1SAX J1218.9+2958 in the quasar regime. The X-ray spectrum shows no evidence for a scattered component or for a soft component.

The colours indicate that the central AGN in 1SAX J1218.9+2958 accounts for at least 50% of the K band emission regardless of the assumed host morphology. This has important implications for photometric redshift determinations for faint sources which assume that emission is dominated by a host galaxy.

Comparing X-ray and optically derived values for the column density intrinsic to 1SAX J1218.9+2958, we deduce that the ratio of extinction to X-ray absorption in 1SAX J1218.9+2958 is 0.1 – 0.7 times that expected from a Galactic extinction curve.

ACKNOWLEDGEMENTS

Based on observations obtained with *XMM-Newton*, an ESA science mission with instruments and contributions funded by ESA Member States and the USA (NASA). This publication makes use of data products from the Two Micron All Sky Survey, which is a joint project of the University of Massachusetts and the Infra-red Processing and Analysis Center/California Institute of Technology, funded by the National Aeronautics and Space Administration and the National Science Foundation. This research made use of ALFOSC, which is owned by the Instituto de Astrofísica de Andalucía (IAA) and operated at the Nordic Optical Telescope under agreement between IAA and the NBIfAFG of the Astronomical Observatory of Copenhagen.

REFERENCES

- Alexander D.M. et al., 2002, *AJ*, 123, 1149
 Akiyama M., et al., 2000, *ApJ*, 532, 700
 Antonucci R.R.J. & Miller J.S., 1985, *ApJ*, 297, 621
 Barger A., Cowie L., Mushotzky R. & Richards E., 2001, *ApJ*, 121, 662
 Brandt W.N. et al., 2001, *AJ*, 122, 2810
 Comastri A., Setti G., Zamorani G. & Hasinger G., 1995, *A&A*, 296, 1
 Comastri A. et al., 2001, *MNRAS*, 327, 781
 Crawford C.S. et al., 2002, *MNRAS*, 333, 809
 Dickey J.M. & Lockman F.J., 1990, *ARA&A*, 28, 215
 Fabian A.C. & Iwasawa K., 1999, *MNRAS*, 303, L34
 Fioc M. & Rocca-Volmerange B., 1999, *A&A*, 351, 869
 Fiore F. et al., 1999, *MNRAS*, 306, L55
 Fitzpatrick E.L., 1999, *PASP*, 111, 63
 Franceschini A. et al., 2001, *A&A*, 378, 1
 Francis P.J. et al. 1991, *ApJ*, 373, 465
 George I.M. & Fabian A.C., 1991, *MNRAS*, 249, 352
 Gandhi P., Crawford C.S. & Fabian A.C., 2002, *MNRAS*, 337, 781
 Gilli R., Salvati M. & Hasinger G., 2001, *A&A*, 366, 407
 Hasinger G. et al., 1998, *A&A*, 329, 482
 Hasinger G. et al., 2001, *A&A*, 365, L45
 Hutchings J.B., Crampton D. & Campbell B., 1984, *ApJ*, 280, 41
 Kinkhabwala A. et al., 2002, *ApJ*, 575, 732
 Koekemoer A.M. et al., 2002, *ApJ*, 567, 657
 La Franca F. et al., 2002, *ApJ*, 570, 100
 Laor A. & Draine B.T., 1993, *ApJ*, 402, 441
 Laor A. et al., 1997, *ApJ*, 477, 93
 Leahy D.A. & Creighton J., 1993, *MNRAS*, 263, 314
 Lehmann I. et al., 2000, *A&A*, 354, 35
 Lehmann I. et al., 2001, *A&A*, 371, 833
 Maccacaro, T., Perola G.C. & Elvis M., 1982, *ApJ*, 257, 47
 Mainieri V. et al., 2002, *A&A*, 393, 425
 Maiolino R. et al., 2000, *A&A*, 355, L47
 Maiolino R. et al., 2001a, *A&A*, 365, 28
 Maiolino R., Marconi A. & Oliva E., 2001b, *A&A*, 365, 37
 Mannucci F. et al., 2001, *MNRAS*, 326, 745
 Matt G., Perola G.C. & Piro L., 1991, *A&A*, 247, 25
 McHardy I.M. et al., 1998, *MNRAS*, 295, 641
 Nandra K., George I.M., Mushotzky R.F., Turner T.J. & Yaqoob T., 1997, *ApJ*, 477, 602
 Page M.J., Mittaz J.P.D. & Carrera F.J., 2000, *MNRAS*, 318, 1073
 Page M.J., Mittaz J.P.D. & Carrera F.J., 2001, *MNRAS*, 325, 575
 Page M.J. et al., 1997, *MNRAS*, 291, 324
 Reichert G.A., Mushotzky R.F., Petre R. & Holt S.S., 1985, *ApJ*, 296, 69
 Roche N. et al., 2002, *MNRAS*, 337, 1282
 Rosati P. et al., 2002, *ApJ* 566, 667
 Sako M., Kahn S.M., Paerels F. & Liedahl D.A., 2000, *ApJ*, 543, L115
 Stevens J.A. et al., 2003, *MNRAS*, accepted
 Tozzi P., et al., 2001, *ApJ*, 562, 42
 Turner M.J.L. et al., 2001, *A&A*, 265, L27
 Ueda Y., et al., 1999, *ApJ*, 518, 656
 Vignali C., Comastri A., Fiore F. & La Franca F., 2001, *A&A*, 370, 900
 Watson M. et al., 2001, *A&A*, 365, L51
 Weingartner J. & Murray N., 2002, *ApJ*, 580, 88
 Wilman R., Fabian A. & Nulsen P., 2000, *MNRAS* 319, 583